Communication

Synthetic Nanomotors in Microchannel Networks: Directional Microchip Motion and Controlled Manipulation of Cargo

Jared Burdick, Rawiwan Laocharoensuk, Philip M. Wheat, Jonathan D. Posner, and Joseph Wang

J. Am. Chem. Soc., **2008**, 130 (26), 8164-8165 • DOI: 10.1021/ja803529u • Publication Date (Web): 06 June 2008

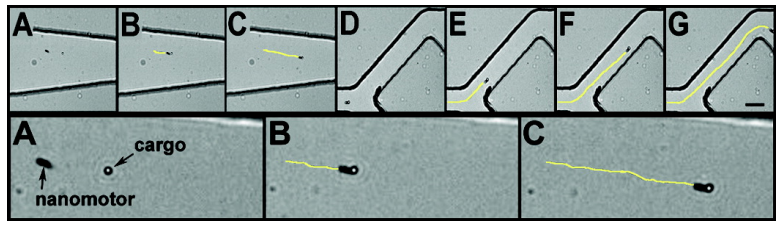

More About This Article

Additional resources and features associated with this article are available within the HTML version:

- Supporting Information
- Links to the 3 articles that cite this article, as of the time of this article download
- Access to high resolution figures
- Links to articles and content related to this article
- Copyright permission to reproduce figures and/or text from this article

View the Full Text HTML

J|A|C|S
COMMUNICATIONS

Published on Web 06/06/2008

Synthetic Nanomotors in Microchannel Networks: Directional Microchip Motion and Controlled Manipulation of Cargo

Jared Burdick,[†] Rawiwan Laocharoensuk,[‡] Philip M. Wheat,[†] Jonathan D. Posner,[†,*] and Joseph Wang[‡,*]

Biodesign Institute, Departments of Mechanical & Aerospace Engineering, Chemical Engineering, and Chemistry & Biochemistry, Arizona State University, Tempe, Arizona 85287-5801

Received May 12, 2008; E-mail: jonathan.posner@asu.edu; joseph.wang@asu.edu

Ⓦ This paper contains enhanced objects available on the Internet at http://pubs.acs.org/jacs.

Controlled motion and transport of nanoscale objects within microfluidic channels represent a critical step toward designing integrated microdevices, powered by autonomous transport (instead of pressure or electrical-driven bulk flow).[1,2] Biological motors, such as kinesin-powered biomolecular shuttles, have shown considerable promise for enhancing the functionality of laboratory-on-a-chip devices.[2] However, the use of biological motors for directional microchip transport and delivery suffers from low speed transport, requires biomolecular patterning, and fixed channel designs to guide the motion. Analogous efforts involving the use of nonbiological (synthetic) nanomotors for directional microchip transport and delivery have not been reported.

Considerable efforts have recently been devoted to the development of synthetic nanomachines.[3–8] In particular, chemically powered bimetal Pt−Au nanowires exhibit autonomous self-propulsion due to electrocatalytic decomposition of an hydrogen peroxide fuel.[3–6] We demonstrated that the incorporation of carbon-nanotubes (CNT) into metal nanowire motors leads to a dramatic increase of their velocity.[7] Sen's group just reported on the movement of sphere-loaded functionalized Pt−Au−Ni-polymer nanowires in free hydrogen peroxide solutions.[8]

In this Communication we demonstrate the directed motion of catalytic nanomotors and their cargo transport and manipulation capabilities along predetermined paths within microchannel networks. We eliminate the requirement for functionalization of the nanowire by making use of the magnetic properties of a nickel segment for guiding and sorting of nanomotors through various junctions of the microfluidic network at high speeds up to 40 μm/sec. In addition, the magnetic segments enable dynamic loading and transport of spherical magnetic cargo throughout the microchannel network, along with a controlled cargo release. The high cargo-towing forces and speed of CNT-based nanomachines indicate promise for demanding microchip applications.

The ability of a nanomotor to travel on a predetermined path is an important aspect of the integration of nanomotors into microfluidic networks. Magnetically directed motion of nickel-containing nanowire motors was demonstrated earlier in free solutions,[6,7] but not in connection to guided motion within microchannels. Directed motion of chemically powered Au/Ni/Au/Pt-CNT nanowires within a microchannel network is illustrated in Figure 1 with channels containing 5 wt% H_2O_2 and no bulk fluid flow. A weak external magnet was used for sorting the nanomotors in each of the junctions of the microfluidic network, without contributing to the nanomotors speed. For example, Figure 1A (and the corresponding video 1) illustrates a 2 μm long Au/Ni/Au/Pt-CNT nanomotor traveling in an hourglass pattern along a 700 μm long preselected path in a symmetric central portion of the microchannel network over a 70 sec period. Figure 1B (and the second part of video 1) further illustrates the directional manipulation of the nanomotors within the microchannel network. Four predetermined paths (a−d), starting from the same starting point (SP), illustrate the dexterity of the CNT-based nanomotors and the magnetic sorting in different junctions. It should be noted that the same nanowire was traveling continuously in all four paths of Figure 1B (as well as returning to the same starting point) for more than an hour.

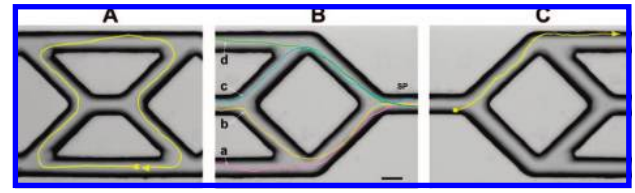

Figure 1. Tracks of directed nanomotor movement within a microfabricated channel network. (A) Motion of an Au/Ni/Au/Pt-CNT nanomotor maneuvering around the central portion of a PDMS microstructure; (B) motion of the same nanowire over four different paths (a−d) beginning from the same starting point (SP); (C) motion of a nanomotor in a mixed peroxide/hydrazine fuel. Fuels, 5 wt% H_2O_2 (A,B); 2.5 wt% H_2O_2/0.15 wt% hydrazine (C). Scale bar, 25 μm.

Ⓦ video 1, illustrating the nanomotor traveling in an houglass pattern and four predetermined paths, is available.

Ⓦ video 2, showing an increase in speed with the addition of hydrazine to the fuel is available.

While the speed of CNT-doped nanomotors in free solutions of 5 wt % H_2O_2 is ca. 40 μm/sec, their speed in the peroxide-containing PDMS microchannel system is reduced dramatically to around 10 μm/sec. The exact reason for the slower speed within the microfluidic network is not well understood but preferential absorption of H_2O_2 into the PDMS is suspected. Note that the speed of CNT-based nanowires within microchannels is still greater than that reported for the undoped nanomotors in free 5 wt % peroxide solutions (outside of channels).[3–6] A dramatic increase in the speed of the CNT nanomotors within the microchannels, to greater than 40 μm/sec, can be achieved by adding hydrazine to the peroxide fuel (Figure 1C and corresponding video 2). The nanomotor travels quickly over an entire 250 μm path in 6 sec in this mixed fuel. Analogous movement in peroxide/hydrazine free solutions (outside channels) resulted in an average speed of 94 μm/sec.[7]

Controlled manipulations of cargo within microchannel networks hold considerable promise for a wide range of microchip applications, including separation and enrichment. While kinesin-powered bioshuttles have been proposed for controlling microscale transport and delivery of cargo in hybrid biological/engineering microsystems,[2] analogous microchip cargo-manipulation using man-made nanomotors

[†] Department of Mechanical & Aerospace Engineering.
[‡] Biodesign Institute, Departments of Chemical Engineering, and Chemistry & Biochemistry.

10.1021/ja803529u CCC: $40.75

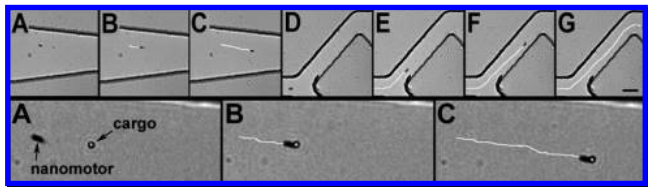

Figure 2. Optical microscopy images of the dynamic loading of a Au/Ni/Au/Pt-CNT nanomotor with a 1.3 μm diameter magnetic microparticle cargo (A−C) and transport it through PDMS microchannels (D through G). Scale bar of panel G, 25 μm. Bottom images in panels A−C are magnified by 3.5 times that of the top images panels A−G.

Ⓦ video 3, demonstrating the ability of the CNT-based nanomotor to load a spherical cargo and transport it along predetermined paths in the channel network is available.

has not been reported. The optical micrographs shown in Figure 2 demonstrate the ability of the CNT-based nanomotor to load a spherical cargo and transport it along predetermined paths in the channel network (A−G). These seven sequential frames are taken from video 3. These images (and video) demonstrate the movement of the nanomotor toward the 1.3 μm diameter spherical (iron-oxide coated polystyrene bead) cargo (A), the magnetic "en route loading" of the cargo by the nanomotor (B), and subsequent travel of the cargo-loaded nanomotor over defined preselected paths in the microfabricated channels (C−G). The time between acquired frames and distance traveled by the loaded nanomotors are 58 msec and 0.5 μm, respectively, translating to a cargo delivering velocity of ca. 9 μm/sec. The reduced speed of the cargo-loaded nanomotor compared to that ($\sim$15 μm/sec) of the solitary CNT-based nanomotor without the cargo (A), reflects the viscous drag on the microsphere. The cargo-loaded velocity of our CNT loaded nanomotors within microchannels is similar to that common to unloaded conventional Pt−Au nanowires in free solutions.[3–7] Sen and co-workers[8] recently reported Pt−Au nanomotors carrying 2.1-μm diameter polystyrene (PS) microspheres in free solutions at a speed of 3.5 μm/sec and an immeasurable speed upon binding of a larger 3.3 μm PS cargo. While this same study requires extra steps for preloading the cargo,[8] we rely here on the magnetic properties of the nickel segment for the dynamic loading of large magnetic microspheres.

As indicated from the dependence of the speed of the cargo-loaded CNT nanomotors upon the diameter of the spherical cargo (Figure 1 in Supporting Information), the nanomotor velocity decreases from 11 to 4 μm/sec upon increasing the cargo size from 1.3 to 4.3 μm, respectively. Figure 1 SI also shows a theoretical prediction of the nanomotor velocity with bound-spherical cargo of varying sizes based on Stokes law of drag at low Reynolds numbers. By knowing the speed and particle size for a nanomotor/particle pair, the force exerted by a nanomotor (F_{nm}) can be estimated to be 0.16 pN. This assumes that F_{nm} is balanced by the Stokes drag force on the cargo (F_d): $F_d = F_{nm} = 6\pi\mu\mathbf{U}a$(where μ is the fluid viscosity, $\mathbf{U}$ the velocity of the nanomotor/particle pair and a is the particle radius). Substantially smaller forces ($\sim$0.04 pN) have been reported for conventional (undoped) Pt−Au nanowires.[5] The larger cargo-towing forces of the CNT-based nanomotors allow transport of larger cargo at a faster speed compared to common Pt−Au nanowires (e.g., 4 μm/sec for the 4.3 μm cargo compared to 3.5 μm/sec for the 2.1 μm cargo,[8] respectively).

The magnetic properties of the Au/Ni/Au/Pt-CNT nanomotor can also be exploited for executing a controlled release of the magnetic-spherical cargo. On-demand cargo release is accomplished by exploiting the weak interaction between the nickel segment within the nanomotor and the magnetic polystyrene beads. A fast change in the direction of the nanomotor (through rapid 180° rotation of the external magnet) thus causes release of the magnetic cargo when the viscous fluid drag on the particle exceeds the magnetic force between the

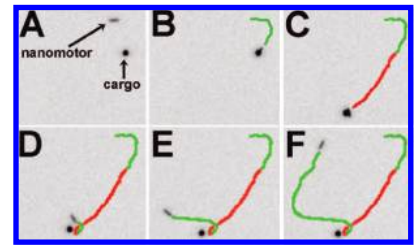

Figure 3. Sequential optical microscopy images (A−F) of an en-route cargo pickup, transport, and release by an Au/Ni/Au/Pt-CNT nanomotor. Green and red traces denote the path traveled by the nanomotor and the cargo-loaded nanomotor, respectively: (A and B) the manipulation toward and pickup of cargo by a nanomotor; (C) subsequent transport of the cargo by the nanomotor; (D) release of the cargo; (E and F) motion of the nanomotor after the cargo release. Fuel, 5 wt % hydrogen peroxide.

Ⓦ video 4, illustrating an entire cargo "load, drag, and drop" operation is available.

Ⓦ video 5, illustrating the control of speed in connection to "stop-turn-and-go" operations is available.

nanowire and the particle. The optical images of Figure 3 (and video 4) illustrate an entire cargo "load, drag, and drop" operation (A−B, C, D, respectively), followed by the movement of the unloaded nanomotor away from the released cargo (E,F).

The nickel segment within the nanomotor also allows control of their speed in connection to "stop-turn-and-go" operations (Figure 2 in SI and video 5). Here the nanowire motion is stopped for 5 sec while turning $\sim$90° in both a clockwise and counter-clockwise direction. This was accomplished by modulating the distance of two square external dipole magnets and changing the direction of the magnetic field (by rotating the magnet) while the nanomotor is stopped. The corresponding video illustrates that the directional movement of the nanomotor is stopped in the presence of the strong magnetic field and renewed upon switching to a weak field. Reversible changes in the nanomotor speed are observed (in the bottom of Figure 2 in SI) during repetitive "on/off" cycles.

In conclusion, we have demonstrated the operation and attractive performance of synthetic nanomotors within microchannel networks, including their directed motion and cargo manipulations along predetermined paths. Synthetic nanomachines pave the way to integrated functional microdevices powered by autonomous transport and perform a series of tasks.

Acknowledgment. The authors acknowledge grants from NSF (Grant CHE 0506529 to J.W. and CARRER Award CBET-0747917 to J.D.P.) and fellowships from the Thai government to R.L. and NSF to P.M.W.

Supporting Information Available: Related protocols, instrumentation, reagents, additional data. This material is available free of charge via the Internet at http://pubs.acs.org.

References

(1) van den Heuvel, M. G.; Dekker, C. *Science* **2007**, *317*, 333–336.
(2) (a) Clemmens, J.; Hess, H.; Doot, R.; Matzke, C. M.; Bachand, G. D.; Vogel, V. *Lab Chip* **2004**, *4*, 83–86. (b) Hiratsuka, Y.; Tada, T.; Oiwa, K.; Kanayama, T.; Uyeda, T. P. *Biophys. J.* **2001**, *81*, 1555–1561.
(3) Paxton, W. F.; Kistler, K. C.; Olmeda, C. C.; Sen, A.; St Angelo, S. K.; Cao, Y.; Mallouk, T. E.; Lammert, P. E.; Crespi, V. H. *J. Am. Chem. Soc.* **2004**, *126*, 13424–13431.
(4) (a) Fournier-Bidoz, S.; Arsenault, A.; Manners, I.; Ozin, G. A. *Chem. Commun.* **2005**, *4*, 441–443. (b) Ozin, G. A.; Manners, I.; Fournier-Bidoz, S.; Arsenault, A. *Adv. Mater.* **2005**, *17*, 3011–3018.
(5) Paxton, W. F.; Sen, A.; Mallouk, T. E. *Chem.—Eur. J.* **2005**, *11*, 6462–6470.
(6) Kline, T. R.; Paxton, W. F.; Mallouk, T. E.; Sen, A. *Angew. Chem., Int. Ed* **2005**, *44*, 744–746.
(7) Laocharoensuk, R.; Burdick, J.; Wang, J. *ACS Nano* **2008**, *2*, 1069–1075.
(8) Sundararajan, S.; Lammert, P. E.; Zudans, A. W.; Crespi, V. H.; Sen, A. *Nano Lett.* **2008**, *8*, 1271–1276.

JA803529U